

## ANALYSIS OF REFLECTOR AND HORN ANTENNAS USING MULTILEVEL FAST MULTIPOLE ALGORITHM

Alex Heldring<sup>\*</sup>, Juan M. Rius<sup>†</sup>, Angel Cardama<sup>†</sup> and Leo P. Ligthart<sup>\*</sup>

<sup>\*</sup>International Research Centre for Telecommunications and Radar,  
Delft University of Technology  
Mekelweg 4, 2628 CD Delft, The Netherlands  
Email: [irctr@its.tudelft.nl](mailto:irctr@its.tudelft.nl)

<sup>†</sup>Universitat Politècnica de Catalunya,  
Dept. of Signal Theory and Communications,  
C/ Jordi Girona 1-3, 08034 Barcelona, Spain  
Email: [heldring@volor.upc.es](mailto:heldring@volor.upc.es)

**Key words:** Computational Electromagnetics, Antennas, Method of Moments, Fast Multipole Algorithm.

**Abstract.** *The MultiLevel Fast Multipole Algorithm (MLFMA) has been implemented in a Method of Moments code for arbitrarily shaped metal surfaces discretized in Rao, Wilton and Glisson (RWG) basisfunctions. The accuracy of the algorithm has been assessed by comparing the results with the exact theoretical solution for a Perfectly Conducting Sphere. Subsequently it has been applied to a parabolic reflector and an X-band horn, comparing the results with measurements. Symmetric properties of the antennas have been exploited and an efficient Incomplete LU preconditioner for the iterative solver has been applied.*

## 1 INTRODUCTION

Electrically large reflectors and horn antennas are usually analysed with high frequency approximation techniques (Physical Optics, Physical Theory of Diffraction) which can adequately predict parameters like the gain and the beamwidth. Sometimes, however, very accurate predictions of the entire radiation pattern are required. An example is the TARA atmospheric radar system currently under construction at the IRCTR in Delft, The Netherlands [1]. One of the requirements for the TARA system, which involves two parabolic reflectors of approximately 30 wavelengths in diameter, is a far sidelobe level of  $-80$  dB. To achieve this, the reflectors are shielded by large conical metallic rims. A accurate numerical simulation of this structure is a most welcome optimisation tool. The most reliable and generally applicable method to obtain such accuracy is to solve the associated integral equation by way of the method of moments (MoM). Until recently, the excessive computational requirements prohibited this approach to problems of this size, but the advent of very efficient acceleration methods for the numerical solution of electromagnetic integral equations and the fast growth of computer capacity has brought them within reach. Among the most efficient acceleration methods is the Multilevel Fast Multipole Algorithm or MLFMA [2]. The present paper gives a short theoretical description of the MLFMA, describes an implementation in an existent MoM code for perfectly conducting objects of arbitrary shape, and assesses its performance by comparisons to an exact theoretical solution for a metal sphere and to measured antenna results. The necessary improvements to tackle the TARA problem are shortly addressed in the conclusion.

## 2 THEORY

### 2.1 Method of Moments

The appropriate integral equation to describe large open objects like antenna reflectors is the Electric Field Integral Equation (EFIE). The object is considered built up of electrically thin sheets ( $d \ll \lambda$ ) and the calculated quantity is the sum of the induced surface currents on both sides, due to a known incident electric field. A finite set of basis functions is chosen to represent the current over the surface, and a set of testing functions is chosen to weigh the incident field over the surface. In the present case both basis and testing functions are Rao, Wilton and Glisson triangular rooftop basis functions [3]. This leads to a matrix representation

$$[-\mathbf{E}_{\text{inc}}] = [\mathbf{Z}][\mathbf{I}], \quad (1)$$

where  $[-\mathbf{E}_{\text{inc}}]$  and  $[\mathbf{I}]$  are vectors of length  $N$  representing the incident field and the current respectively, and  $[\mathbf{Z}]$  is an  $N$  by  $N$  matrix with elements given by (three dimensional vectors are represented by lower case boldface characters)

$$Z_{nm} = \frac{1}{j\omega\epsilon_0} \iint \mathbf{f}_n(\mathbf{x}) \cdot (k_0^2 - \nabla'^2) g(\mathbf{x}, \mathbf{x}') \mathbf{f}_m(\mathbf{x}') d\mathbf{x} d\mathbf{x}'. \quad (2)$$

In (2),  $k_0$ ,  $\omega$  and  $\epsilon_0$  are the wave number, angular frequency and free space permittivity, respectively. The vector functions  $\mathbf{f}_n(\mathbf{x})$  are the basis and testing functions. The double integration is over the domain of the basis and testing functions, and  $g$  is the scalar free space Green's function. Equation (1) must be solved for  $[\mathbf{J}]$ , after which the radiation pattern can be obtained straightforwardly. Solving (1) directly has a computational complexity of  $N^3$ . Alternatively, an iterative algorithm can be employed to obtain an approximate solution. A common iterative algorithm is the Biconjugate Gradient (BiCG) method, which takes two matrix-vector products ( $2N^2$  operations) per iteration step, but generally converges to sufficient accuracy in far less than  $N$  steps. Nevertheless, both computing time and storage become prohibitive once the object surface exceeds certain limits.

## 2.1 Multilevel Fast Multipole Algorithm

The MLFMA yields an approximate representation of the matrix  $[\mathbf{Z}]$  in (1). The accuracy of the approximation can be chosen at will, to be traded against the computational costs. The basis of the algorithm is an expansion of the Green's function around the source and field points [2]

$$g(\mathbf{r}_c + \mathbf{d}_n - \mathbf{d}_m) = \frac{e^{-jk_0|\mathbf{r}_c + \mathbf{d}_n - \mathbf{d}_m|}}{|\mathbf{r}_c + \mathbf{d}_n - \mathbf{d}_m|} \approx \frac{-jk_0}{4\pi} \int e^{-j\hat{\mathbf{k}} \cdot \mathbf{d}_m} T(\hat{\mathbf{k}}, \mathbf{r}_c) e^{+j\hat{\mathbf{k}} \cdot \mathbf{d}_n} d^2\hat{\mathbf{k}}, \quad (3)$$

$$T(\hat{\mathbf{k}}, \mathbf{r}_c) = -\sum_{l=0}^L j^l (2l+1) h_l^{(2)}(k_0 r_c) P_l(\hat{\mathbf{k}} \cdot \mathbf{r}_c). \quad (4)$$

In (3), the integration is over the unit sphere. The expansion is valid for  $r_c \gg d_n$  and  $r_c \gg d_m$ . In (4),  $h_l^{(2)}$  is the spherical Hankel function of the second kind of order  $l$  and  $P_l$  is Legendres polynome of order  $l$ .

The first step is to subdivide the basis functions into geometrical sub groups. To this aim, the object is enclosed inside a box. The box is then recursively split into eight smaller boxes, down to a fixed level of smallest boxes (the resulting structure is called an octal tree). At every level, the interactions between basis functions inside 'nearby' boxes (typically touching boxes) is represented by the interactions between their 'child boxes'. At the lowest level, these are simply the interactions between basis functions, as in (2). For the interactions between far enough boxes, the submatrix  $[\mathbf{Z}_{s,f}]$ , where the subscripts  $s$  and  $f$  denote the source and field boxes respectively, is replaced by the product

$$[\mathbf{Z}_{s,f}] \approx \sum_i [\mathbf{V}_f^\dagger] [\mathbf{T}_{s,f}] [\mathbf{V}_s]. \quad (5)$$

The substitution (5) is obtained using (3) in (2), with an appropriate discretisation of the integral in (3).  $[V]$  is a plane wave expansion of the basis functions around the box centre; the summation index  $i$  is over the three spatial components plus the derivative of the basis functions. It represents the inner product in (2).  $[T]$  is a diagonal matrix with the factors defined in (4). The number of directions on the unit sphere necessary to represent the interaction depends linearly on the geometrical size of the concerned boxes. Therefore, twice as many directions are needed with every step up the octal tree. They need not be recomputed directly from the basis functions however. Instead, they can be found using shifting (to the new group centre) and interpolation of the ‘child box’ plane wave expansions,

$$[V^{L+1}] \approx \sum_c [Q_L][W_L][V^L], \quad (6)$$

where  $L$  denotes the level in the octal tree. The summation index  $c$  is over all the ‘child boxes’.  $[Q_L]$  is the (diagonal) shifting operator, and  $[W_L]$  interpolates to a new set of unit vectors on the sphere. If a sparse (local) approximation scheme is used, the overall storage requirement and the computational complexity of a matrix-vector product is reduced to order  $N \log(N)$ .

The error in the multipole approximation depends on three parameters, the order of the expansion  $L$  in (4), the number of multipole directions and the minimum distance between boxes. Furthermore, the overall error also depends on the interpolation operator  $[W]$  that is used. The first three are linked. Reference [2] presents them as functions of a single parameter  $p$ . A choice of  $p=5$  yields 32 bits accuracy, but if an error in the surface current of 10 – 25% is acceptable (this typically leads to an error of less than 1% in the far field pattern)  $p=1.5$  is sufficient. In the latter case, a low order interpolation scheme (based on second degree polynomials) is adequate. For 32 bits precision, a high order (global) interpolation is necessary, leading to full interpolation matrices  $[W]$ . For this case, fast interpolation operators based on FFT and a Fast Legendre Transform have been proposed [4]. Since these have an  $N \log(N)$  complexity, this leads to an overall complexity of  $N \log^2(N)$  per matrix-vector product.

Another issue of importance is the convergence of the BiCG algorithm. The convergence speed depends on  $N$  and generally, it is unacceptably slow for large problems ( $N > 1e4$ ). Therefore, a preconditioned system

$$[M^{-1}][-\mathbf{E}_{inc}] = [M^{-1}][Z][J] \quad (7)$$

with an advantageous choice for  $[M]$ , is solved instead. Good results are obtained when taking for  $[M]$  a sparse approximation of  $[Z]$ , retaining only the 50 largest elements per row. This is easily obtained from  $[N]$ . Then  $[M^{-1}]$  is computed as an incomplete LU decomposition (ILU) of  $[M]$ , where the threshold is chosen to obtain as large as possible  $[L]$  and  $[U]$ , given the available computer storage.

### 3 RESULTS

#### 3.1 Perfectly Conducting Sphere

The accuracy of the MLFMA was assessed by comparing the computed RCS of a large conducting sphere (diameter  $D = 8.84 \lambda$ ) with the exact (Mie series) result. The sphere was discretised into 32768 triangular facets, yielding 49152 RWG basis functions. The MLFMA precision factor was set to  $p=1.5$  with second degree polynomial interpolation. The total size of the MLFMA decomposition was 604 MB, plus a 77 MB ILU preconditioner. The MLFMA matrices are swapped from the hard disk in chunks during the iteration. Total computing time was 6h 49min on a Pentium II 400 MHz, 256 MB RAM (the convergence to 1% relative error took 13 iterations, 12.5min per iteration). The relative RMS error in the current was 11%, in the RCS: 0.8%. Fig. 1 shows the RCS.

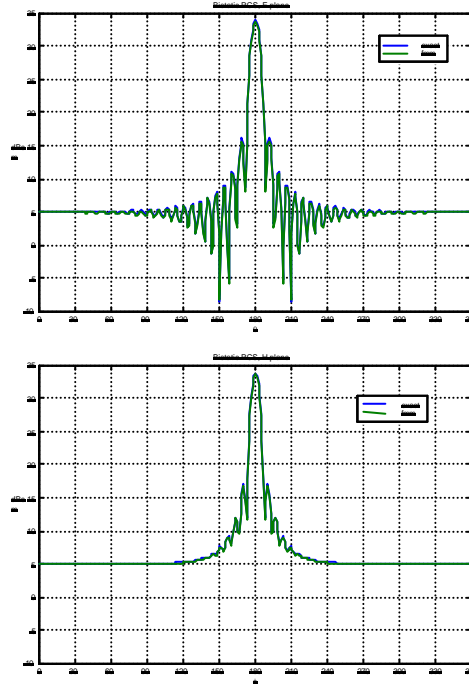


Figure 1: RCS of PEC sphere, diameter  $8.84\lambda$ , 49152 unknowns

### 3.2 Parabolic Reflector

Subsequently, a small parabolic reflector was modelled and compared with measurements. The specifications of the reflector and the simulation are given in Table 1.

Diameter	$5 \lambda$
F/D	0.376
Feeding	Dipole + $\frac{1}{2} \lambda$ circular disk
Number of RWG basis functions	11384
Using 4-fold symmetry	2954

Table 1 : Specifications of Parabolic Reflector

The reflector was fed with an infinitesimal dipole in the focal point, backed by a  $\frac{1}{2} \lambda$  circular disk placed at  $\frac{1}{2} \lambda$  above the focal point. Using the 4-fold symmetry of the problem, the MoM linear system could be solved by direct inversion. This allowed for a comparison of direct MoM and MLFMA. The MLFMA decomposition was done with precision factor  $P=1.5$  and 2<sup>nd</sup> degree polynomial interpolation. It contained 5 levels. The difference in the computed surface current between MLFMA and direct MoM was smaller than 3%. Fig. 2 shows the radiation patterns obtained from the computed currents compared with the measured pattern. The direct inversion took 59 minutes (of which 37 minutes for building the impedance matrix), the MLFMA computation took 24 minutes (of which 15 for building the MLFMA decomposition and a 7 MB ILU preconditioner).

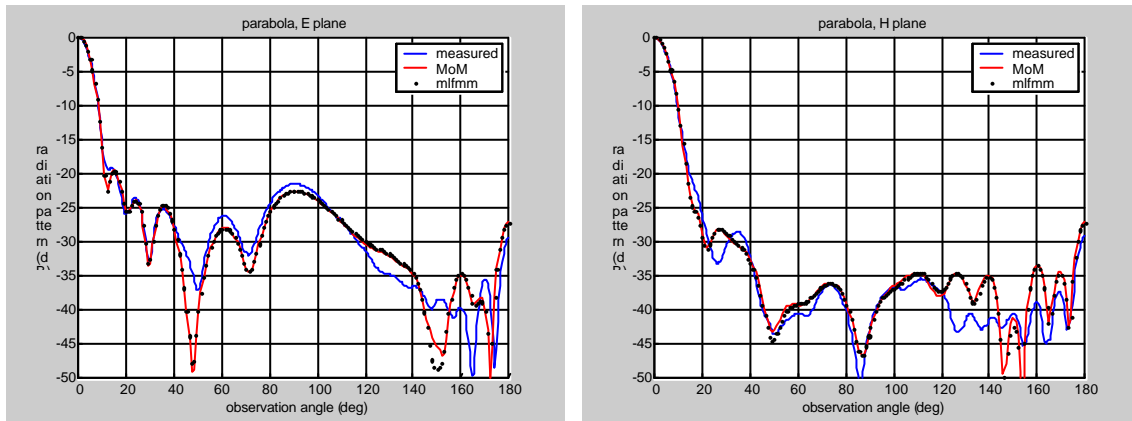


Figure 2: Radiation pattern of parabolic reflector, diameter  $5\lambda$ , 11384 unknowns

### 3.3 X-band Horn

The next simulation concerned an X-band horn with the specifications described in Table 2.

Aperture	$3 \times 4 \lambda$
Horn height	$8.2 \lambda$
Waveguide section	$0.8 \times 0.3 \times 2 \lambda$
Feeding	Dipole in centre of waveguide
RWG basisfunctions	69000 (17781 using symmetry)

Table 2 : Specifications of X-band Horn

4-fold symmetry was employed. The MLFMA decomposition had precision parameter  $P=2$  and 4<sup>th</sup> degree polynomial interpolation. The decomposition had 7 levels. The entire MLFMA decomposition had a size of 1.3 GB. A 150 MB ILU preconditioner was used. The matrix setup time was 11h6min, the iteration (to 1% relative error) took 22 steps of about 13min each adding up to 4h40min. Fig. 2 shows the MLFMA computed, Aperture Theory computed and measured radiation patterns. Beyond 40 degrees off boreside, where Aperture Theory fails, the MLFMA pattern still matches well with the measurement as the figure shows. Fig. 3, a shows the horn with the computed current distribution (amplitude).

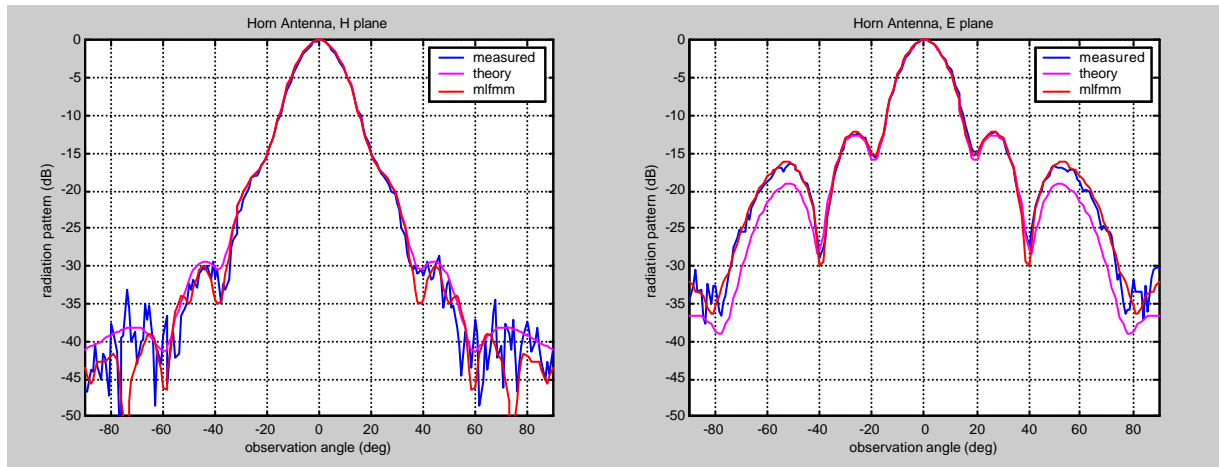


Figure 3: Radiation pattern X-band horn, aperture  $4 \times 3 \lambda$ , 69000 unknowns

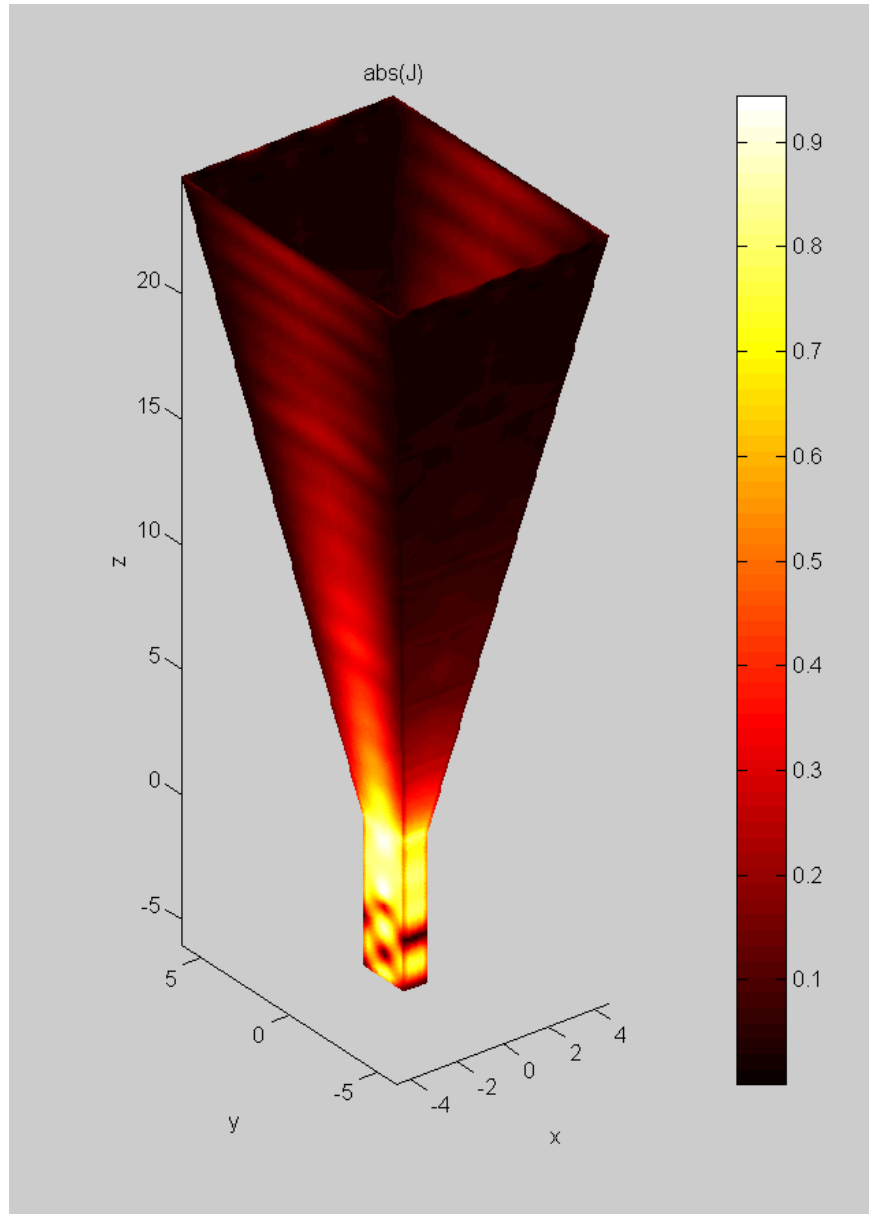


Figure 4: X-band horn, MLFMA computed surface current amplitude



## 4 CONCLUSIONS

The presented results show that the MLFMA combined with the EFIE and Method of Moments yields good results for large metal objects, two problems of well over 10.000 unknowns have been presented. In its present stage of development problems of over 100.000 unknowns should not pose any problems on a common PC like the one that has been used here. The size of the MLFMA decomposition is not a fundamental limitation, due to the hard disk swapping. The main bottleneck for larger problems is the preconditioner. Since the Incomplete LU-decomposition needs to be performed in memory, this poses a limit to the size of the preconditioner. Alternative methods of preconditioning, that do not have a size limiting problem, are under investigation.

## REFERENCES

- [1] S.H. Heijnen and L.P. Ligthart, 'TARA: Transportable Atmospheric Radar,' European Microwave Conference, Amsterdam, 1998
- [2] R. Coifman, V. Rokhlin and S. Wandzura, 'The Fast Multipole Method for the Wave Equation: A Pedestrian Prescription,' IEEE A&P Magazine, Vol 35, No 3 June 1993
- [3] R. M. Rao, D. R. Wilton and A. W. Glisson, 'Electromagnetic Scattering by Surfaces of Arbitrary Shapes,' IEEE A&P Magazine, Vol AP-30, No 3, May 1982
- [4] M.F. Gyure and M.A. Stalzer, 'A Prescription for the Multilevel Helmholtz FMM,' IEEE Comp. Sci.& Eng. July-Sept. 1998